PARAMETER ESTIMATION OF FREQUENCY-MODULATED SINUSOIDS WITH THE DISTRIBUTION DERIVATIVE METHOD

Marcelo Caetano

Department of Music
University of California San Diego (UCSD)
La Jolla, CA
mcaetano@ucsd.edu

ABSTRACT

Frequency-modulated (FM) sinusoids are commonly used to model signals in several engineering applications, such as radar, sonar, communications, acoustics, and optics. The estimation of the parameters of FM sinusoids is a challenging problem with a long history in the literature. In this article, we use the distribution derivative method (DDM) to estimate the parameters of FM sinusoids in additive white Gaussian noise. Firstly, we derive the estimation of parameters of the model with DDM. Then, we compare the results of Monte-Carlo simulations (MCS) of DDM estimation of FM signals in additive white Gaussian noise against the state of the art (SOTA) and the Cramér-Rao lower bound (CRLB). DDM estimation of FM sinusoids showed performance comparable to the SOTA with less estimation bias. Additionally, DDM estimation of FM sinusoids is simple and straightforward to implement with the fast Fourier transform (FFT) relative to other approaches in the literature. Finally, DDM estimation has effectively the same computational complexity as the FFT.

1. INTRODUCTION

Nonstationary signals are ubiquitous in several applications, such as radar, sonar, communications, optics, acoustics, and audio processing. In this article, we are interested in a specific class of nonstationary signals commonly called frequency-modulated (FM) sinusoid, which can be expressed as

$$x\left(t\right)=\exp\left\{a_0+j\,\left(b_0+b_1t+b_2\cos\left(\omega_0t-\phi_0\right)\right)\right\},\qquad(1)$$

where a_0 is the constant log amplitude, b_0 is the initial phase of the carrier, b_1 is the carrier angular frequency, b_2 is the modulation index, ω_0 is the modulation angular frequency, and ϕ_0 is the initial phase of the modulation. We want to estimate all the parameters of $x\left(t\right)$ in (1) from a finite number of noisy observations. In audio processing, the signal in (1) can be used to model the classic FM synthesis [1] as well as vibrato [2, 3, 4]. As such, the estimation of the parameters of $x\left(t\right)$ in (1) has applications in the retrieval of FM synthesis parameters from audio [5, 6] as well as vibrato detection and modeling [2, 3, 4]. In the signal processing literature, the signal in (1) is also called hybrid FM-polynomial phase [7, 8, 9, 10], and they appear in applications such as micro-Doppler scattering [11, 12] and precession period estimation [13, 14], among others. As such, the estimation of parameters of FM sinusoids is of great interest.

Copyright: © 2024 Marcelo Caetano et al. This is an open-access article distributed under the terms of the Creative Commons Attribution 4.0 International License, which permits unrestricted use, distribution, adaptation, and reproduction in any medium, provided the original author and source are credited.

Parametric estimation methods typically use an underlying signal model for both the time-varying amplitudes and phases. For example, given the general model for an AM-FM sinusoid

$$x\left(t\right)=\exp\left\{A\left(t\right)+j\,\Phi\left(t\right)\right\}=\exp\left\{L\left(t\right)\right\},\qquad(2)$$

where $A\left(t\right)$ is the instantaneous log-amplitude and $\Phi\left(t\right)$ is the instantaneous phase. The signal $x\left(t\right)$ in (2) is called an AM-FM sinusoid because the amplitude is modulated by $A\left(t\right)$ and the frequency by the first time derivative of $\Phi\left(t\right)$. Assuming that the same underlying model can represent the nonstationary characteristics of both $A\left(t\right)$ and $\Phi\left(t\right)$, we write $L\left(t\right)$ in (2) as

$$L\left(t\right)=\sum_{q=0}^{Q}\alpha_q p_q\left(t\right),\qquad(3)$$

where $\alpha_q=a_q+j\,b_q\in\mathbb{C}$, Q is the model order, and the functions $p_q\left(t\right)$ are *linearly independent* [15]. Replacing (3) in (2) yields the general parametric model for an AM-FM sinusoid

$$x\left(t\right)=\exp\left\{\sum_{q=0}^{Q}\alpha_q p_q\left(t\right)\right\},\qquad(4)$$

which can represent a broad class of signals that are typically classified according to the phase. For example, $p_q\left(t\right)=t^q$, $q\in\mathbb{N}$ gives a *polynomial* phase signal (PPS) [16, 17, 15], where the order Q determines *linear* phase (i.e., stationary) for $Q=1$, *quadratic* phase (i.e., chirp) for $Q=2$, *cubic* phase for $Q=3$, etc. When $Q=1$ and $p_q\left(t\right)=\sin\left(\omega t-\varphi\right)$, we have a *sinusoidal* phase signal [7, 18, 19, 11, 12, 13, 20, 14, 21, 22], whereas $p_q\left(t\right)=\ln\left(t\right)$ gives a *hyperbolic* phase signal [7]. Hybrid phase models are also found in the literature, most commonly hybrid polynomial-sinusoidal phase [23, 7, 10, 24, 8, 9, 25] but also hybrid polynomial-hyperbolic phase [7]. Note that the FM-sinusoid of (1) is a special case of hybrid polynomial-sinusoidal phase obtained when $Q=2$, $p_q=t^q$ for $q=0$ and $q=1$, and $p_q=\cos\left(\omega_0t-\phi_0\right)$ for $q=2$ and also $a_1=a_2=0$.

The estimation of the parameters of (1) is a very challenging problem [5, 6, 23, 7, 25, 8, 8, 24, 9, 10] and most proposed solutions found in the literature require complex estimation procedures with high computational complexity to achieve acceptable performance comparable to maximum likelihood estimation (MLE). MLE is known to asymptotically achieve the Cramér-Rao lower bound (CRLB), but MLE of (1) requires a search procedure in a high-dimensional search space, where the number of parameters determines the dimensionality. So MLE of the parameters of (1) is possible, but it requires computationally demanding nonlinear optimization, which tends to converge to local optima [7] in high-dimensional spaces. Consequently, much research effort has been applied to develop estimation methods that approximate the CRLB at a lower computational cost.

In the literature, we find estimation methods using Kalman filtering [5, 6], variations of the high-order ambiguity function [23, 7], and other techniques such as subspace-based estimation [25] or the Radon transform [8]. Techniques based on phase unwrapping [24, 10] achieve quasi-maximum likelihood (QML) performance via refinement stages. In [10], the parameters of the *coupled* FM signal model are estimated in three stages, **stage 1** gives a *rough* approximation, **stage 2** yields a *refined* estimation, and **stage 3** uses a nonlinear *optimization* procedure initialized with the estimation from **stage 2**, which is biased but close enough to the optimum, to approximate the performance of MLE towards the CRLB. Therefore, [10] is considered to be the state of the art because **stage 3** achieves QML performance.

In this work, we present how to use the distribution derivative method [15] (DDM) to estimate all the parameters of (1). DDM provides efficient estimation with a relatively straightforward implementation and low computational complexity for polynomial phase signals (PPS) of *arbitrary* order [15]. The contribution of this work is the adaptation of DDM to estimate the parameters of FM sinusoids, which is not possible with the original DDM presented in [15].

Section 2 briefly reviews DDM estimation of the parameters of (2) for the general case of (3) [15], section 3 presents the proposed method of estimation of parameters of FM sinusoids with DDM, section 4 presents performance evaluation, followed by the discussion in section 5. Finally, section 6 presents the conclusions and future work.

2. DDM ESTIMATION

The foundations of DDM estimation lie in the theory of distributions in mathematical analysis, which generalizes the concept of functions to include objects such as the Dirac delta [26, 27] with the aid of the test function ψ with compact support U_ψ. Distributions x are interpreted as acting on the test function ψ via integration over the support U_ψ. Notably, the theory of distributions extends the notion of derivative of x, which lies at the core of the DDM. Specifically, we want to analyze the signal $x(t)$ with the test function $\psi(t)$, which is zero outside U_ψ and infinitely differentiable on U_ψ. For such, we use the inner product

$$\langle x, \psi \rangle = \int_{-\infty}^{\infty} x(t)\,\bar{\psi}(t)\,\mathrm{d}t = \int_{U_\psi} x(t)\,\bar{\psi}(t)\,\mathrm{d}t \tag{5}$$

where $\bar{\psi}$ is the complex conjugate of ψ. The *derivative* of x with respect to (w.r.t.) its argument t, which we denote $\dot{x}$, is obtained with the aid of $f(t) = x(t)\,\bar{\psi}(t)$. The derivative of f w.r.t. t is then

$$\dot{f}(t) = \dot{x}(t)\,\bar{\psi}(t) + x(t)\,\dot{\bar{\psi}}(t)\,. \tag{6}$$

Integrating (6) w.r.t t over the support U_ψ yields

$$\int_{U_\psi} \dot{f}(t)\,\mathrm{d}t = \int_{U_\psi} \dot{x}(t)\,\bar{\psi}(t)\,\mathrm{d}t + \int_{U_\psi} x(t)\,\dot{\bar{\psi}}(t)\,\mathrm{d}t. \tag{7}$$

Here we note that $\int_{U_\psi} \dot{f}(t)\,\mathrm{d}t = 0$ because ψ (and therefore f) vanishes at the borders of U_ψ. Then, using the notation for the inner product in (5), we have

$$\langle \dot{x}, \psi \rangle = -\langle x, \dot{\psi} \rangle. \tag{8}$$

Equation 8 allows implicitly taking the derivative of the unknown signal x by differentiating the test function ψ instead. The idea behind DDM [15] is to apply (8) to the signal model of (4) to estimate the model parameters α_p. We note that the derivative of (2) w.r.t t reveals the property

$$\dot{x}(t) = \dot{L}(t)\exp\{L(t)\} = \dot{L}(t)\,x(t)\,, \tag{9}$$

which allows expressing (8) as

$$\langle \dot{L}x, \psi \rangle = -\langle x, \dot{\psi} \rangle. \tag{10}$$

Eq. (10) can be used to derive DDM estimation for any generic AM-FM sinusoid that follow the model from (2). Using $L(t)$ given in (3), we have $\dot{L}(t) = \sum_{q=0}^{Q} \alpha_q \dot{p}_q(t)$, so (9) becomes

$$\dot{x}(t) = \sum_{q=0}^{Q} \alpha_q \dot{p}_q(t)\,x(t)\,. \tag{11}$$

Finally, replacing (11) in (8) gives

$$\sum_{q=0}^{Q} \alpha_q \langle \dot{p}_q x, \psi \rangle = -\langle x, \dot{\psi} \rangle, \tag{12}$$

which is the DDM estimation equation for the signal model in (4). Betser [15] introduced DDM estimation for *polynomial phase signals* (PPS), which comprise a broad class of nonstationary signals whose phase can be locally modeled by a polynomial [16, 17].

2.1. DDM Estimation of Polynomial Phase Signals

Polynomial phase signals (PPS) [16] are obtained when $p_q(t) = t^q$, $q \in \mathbb{N}$ in (3), where $\mathbb{N}$ denotes the non-negative integers. In this case, $\dot{p}_q(t) = q\,t^{q-1}$, $q \in \mathbb{N}_+$, where $\mathbb{N}_+$ denotes the positive integers, and

$$\sum_{q=1}^{Q} \alpha_q \langle q\,t^{q-1} x, \psi \rangle = -\langle x, \dot{\psi} \rangle. \tag{13}$$

Since $\dot{p}_q$ only depends on the argument t and on the power q for PPS, the inner products $\langle \dot{p}_q x, \psi \rangle$ can be computed for any unknown signal x assuming its underlying model is PPS. DDM estimates the PPS parameters α_q as the linear coefficients of a system of equations given by (13). Betser [15] presents a general derivation that can use multiple integral transforms whose kernels respect the conditions for the test function ψ. Additionally, [15] describes how to use the *windowed* discrete Fourier transform (DFT) to compute the inner product of (5) and also to derive the matrix equation whose pseudo-inverse yields estimation of α_q. The next section derives $-\langle x, \dot{\psi} \rangle$ using the *windowed* Fourier transform because of the widespread availability of FFT implementations and effortless adaptability of the method for the short-time Fourier transform (STFT), where each frame is assumed to follow the same underlying model and parameter values that evolve across frames.

2.2. DDM Estimation with the Windowed Fourier Transform

For the *windowed* Fourier transform, $\psi(t) = w(t)\,\mathrm{e}^{j\omega t}$, where $w(t)$ is a tapering window with compact support that is differentiable at least once. Then,

$$\dot{\bar{\psi}}(t) = [\dot{w}(t) - j\omega w(t)]\,\mathrm{e}^{-j\omega t}. \tag{14}$$

Replacing (14) on the right-hand side of (8), we get

$$\langle x, \dot{\psi} \rangle = \langle x, [\dot{w}(t) - j\omega w(t)] \, \mathrm{e}^{-j\omega t} \rangle, \tag{15}$$

$$\langle x, \dot{\psi} \rangle = \langle x, \tau \rangle - j\omega \langle x, \psi \rangle, \tag{16}$$

where we use the shorthand $\tau(t) = \dot{w}(t)e^{j\omega t}$ to define $\langle x, \tau \rangle$ as

$$\langle x, \tau \rangle = \langle x, \dot{w}(t)e^{j\omega t} \rangle. \tag{17}$$

Equation (16) shows that $\langle x, \dot{\psi} \rangle$ only requires computing two windowed Fourier transforms of the signal $x(t)$, namely $\langle x, \psi \rangle$ and $\langle x, \tau \rangle$ defined in (17), which simply uses the first time derivative of the window $w(t)$. Note that $\dot{w}(t)$ can be computed analytically for most commonly used windows (except the rectangular window, which has discontinuities, and the slepian window, which does not have an explicit analytical expression), making the computation of (17) very efficient. It is also worth mentioning that ω in (16) comes from the derivative in (14) and it is simply the frequency from the Fourier kernel in $\psi(t)$.

At this point, we can use (13) and (17) to estimate the parameters of PPS with the DFT as described in [15]. In what follows, we will derive DDM estimation for the FM signal model of (1). We stress that DDM estimation originally presented in [15] is not capable of estimating all the parameters of (1) because DDM formulates parameter estimation as a *linear* system of equations that depend on α_q. Section 3 shows that (1) violates the constraint of *linearity* because (1) contains parameters to be estimated *inside* the argument of the functions $p_q(t)$. Section 3.2 shows how to linearize it with the Jacobi-Anger expansion to use DDM estimation for FM sinusoids with the algorithm presented in Sec. 3.3.

3. HYBRID POLYNOMIAL-SINUSOIDAL ESTIMATION

We are going to use the FM sinusoid model from (1) in (8) written as (10) to derive DDM estimation of (1). Comparison of (1) with (2) yields $L(t) = a_0 + j\,[b_0 + b_1 t + b_2 \cos(\omega_0 t - \phi_0)]$, which gives

$$\dot{L}(t) = j\,\,[b_1 - \omega_0\, b_2 \sin(\omega_0 t - \phi_0)]\,. \tag{18}$$

We replace (18) in (10) to get

$$j\,\,[b_1 \langle x, \psi \rangle - \omega_0\, b_2 \langle \sin(\omega_0 t - \phi_0)\, x, \psi \rangle] = -\langle x, \dot{\psi} \rangle. \tag{19}$$

Equation (19) requires prior knowledge of ω_0 and ϕ_0 to estimate b_1 and b_2, which uses the inner product $\langle \sin(\omega_0 t - \phi_0)\, x, \psi \rangle$. Even though (19) suggests that DDM cannot be used to estimate all the parameters of FM signals, the rest of Sec. 3 is dedicated to explaining how it can be achieved.

3.1. Estimation of the Initial Phase

Let us rewrite (18) as

$$\dot{L}(t) = j\,\,[b_1 - \omega_0\, b_c \sin(\omega_0 t) + \omega_0\, b_s \cos(\omega_0 t)]\,. \tag{20}$$

where $b_c = b_2\,\cos\phi_0$ and $b_s = b_2\,\sin\phi_0$. Now we replace (20) in (12) to get

$$j\,[b_1 \langle x, \psi \rangle - \omega_0 b_c \langle p_s\, x, \psi \rangle + \omega_0 b_s \langle p_c\, x, \psi \rangle] = -\langle x, \dot{\psi} \rangle, \tag{21}$$

where

$$p_c = \cos(\omega_0 t) \quad \text{and} \quad p_s = \sin(\omega_0 t). \tag{22}$$

Estimation of b_1, b_c, and b_s using (21) only depends on ω_0, and ϕ_0 can be easily retrieved from b_c and b_s (see Algorithm 1 for details). Section 3.2 shows how to use the Jacobi-Anger expansion to allow estimation of ω_0 with the DDM.

3.2. Estimation of the Modulation Frequency

The Jacobi-Anger expansion is given by

$$\exp\{j\, b\, \cos(\theta)\} = \sum_{i=-\infty}^{\infty} j^i J_i(b) \exp\{j\, i\, \theta\}, \tag{23}$$

where $J_i(b)$ is the i^{th} Bessel function of the first kind. Therefore, eq (23) allows rewriting (1) as

$$x(t) = \sum_{i=-\infty}^{\infty} j^i J_i(b_2) \exp\{a_0 + j\,[b_0 + b_1 t + i\,(\omega_0\, t - \phi_0)]\}. \tag{24}$$

Note that the i in the exponential in (24) denotes an integer multiple of the modulating frequency ω_0. Thus, eq. (23) expresses the nonlinearity of FM sinusoids as a linear combination of sinusoids at the frequencies $i\,\omega_0$, sometimes called “FM harmonics”, weighed by the amplitudes $J_i(b)$. Once again, comparing (24) with (2), yields $L(t) = a_0 + j\,\,[b_0 - i\,\phi_0 + t\,\,(b_1 + i\,\omega_0)]$, whose derivative w.r.t. t is

$$\dot{L}(t) = j\,\,(b_1 + i\,\omega_0)\,. \tag{25}$$

Replacing (24) in (10) yields

$$b_1 + i\,\omega_0 = j\,\frac{\langle x, \dot{\psi} \rangle}{\langle x, \psi \rangle}, \tag{26}$$

after some algebra. We note that (26) only depends on the carrier frequency b_1 and on the modulation frequency ω_0, and only requires calculation of the inner products with (5) and (16). We also note that $i \in \mathbb{Z}$ according to (23), which is simply the integer multiple of the modulation frequency ω_0 around the carrier frequency b_1. Equation (26) allows *independent* estimation of ω_0 by simply setting $i = 0$ in (26) to estimate b_1 and then $i = 1$ to estimate the modulation frequency ω_0 as explained in section 3.3. But we can further simplify (26) by replacing (16) to get

$$b_1 + i\,\omega_0 = j\,\frac{\langle x, \tau \rangle}{\langle x, \psi \rangle} + \omega, \tag{27}$$

where $\langle x, \tau \rangle$ is calculated with (17) and ω is the frequency variable of the Fourier transform. Equation (27) only requires calculation of two windowed Fourier transforms, instead of three transforms as required in (26).

3.3. DDM Estimation Algorithm

The discrete-time version of the FM signal model in (1) is

$$x(n) = \exp\Big\{a_0 + j\,\,\Big(b_0 + 2\pi\tfrac{f_c}{f_s}n + b_2 \cos\Big(2\pi\tfrac{f_0}{f_s}n - \phi_0\Big)\Big)\Big\}, \tag{28}$$

where a_0 is the constant log amplitude, b_0 is the initial phase in radians, f_c is the carrier frequency in Hertz, f_s is the sampling frequency in samples per second, b_2 is the adimensional modulation index, f_0 is the modulation frequency in Hertz, and ϕ_0 is the modulating initial phase in radians.

We want to estimate a_0, b_0, f_c, b_2, f_0, and ϕ_0 with the DDM from M samples of $x(n)$ in (28), which can also be considered as a frame of the STFT. For such, we use the FFT to calculate (5), (17), and both $\langle p_c\, x, \psi \rangle$ and $\langle p_s\, x, \psi \rangle$ in (21). Note that ω in (16) and (27) becomes $\omega_k = 2\pi\frac{k}{N}$, where N is the size of the FFT and k is the frequency bin. Additionally, the estimation method using the FFT described in [15] only uses K frequency bins around

Algorithm 1 DDM estimation of FM sinusoids

1: Estimate b_1 using (27) with $i = 0$
2: Estimate $b_1 + \omega_0$ using (27) with $i = 1$
3: Calculate ω_0 using steps *1* and *2*
4: Calculate p_c and p_s from (22)
5: Estimate b_1, b_c, and b_s from (21)
6: Estimate $\phi_0 = \arctan\left(\frac{b_s}{b_c}\right)$
7: Estimate $b_2 = \frac{b_s}{\sin(\phi_0)}$ ▷ alternatively, use $b_2 = \frac{b_c}{\cos(\phi_0)}$
8: Estimate α_0 with the least-square estimator from [15]

spectral peaks, which are regions of maximum spectral energy. See section VII in [15] for further details on using the FFT for DDM estimation. Finally, the estimation is done with reference to the center of the frame by multiplying the FFT by $e^{j\,\omega_k\,\frac{M}{2}}$, where M is the window size in samples. *Algorithm* 1 summarizes all the steps required to estimate all parameters of FM signals.

Here, we note that the estimation algorithm 1 contains redundancy in several steps that can be potentially exploited to increase the accuracy of estimation. For example, *steps 1* and *2* can be repeated for other values of i and then *step 3* would use (27) and average the result of the estimation. Additionally, b_1 is estimated in *step 1* and then again in *step 5* as $\Im\{\alpha_1\}$. Also, b_2 can be estimated from either b_c or b_s. We have not exploited redundancy in the current work, which is considered as future work.

4. MS SIMULATIONS AND CRLB COMPARISONS

Djurović *et al.* [10] proposed a method to estimate the parameters of *coupled* FM sinusoids, where the phase of the polynomial component and of the sinusoidal modulation follow the same (polynomial) model and have parameter values coupled by a constant. In this work, only f_c and f_0 are coupled as $f_0 = c_0 f_c$. Following [10], $c_0 = 0.1$ was used. The *coupled* FM signal model in [10] is equivalent to (28) when the order of the polynomial phase and of the sinusoidal modulation are both 1. Here, we also use $f_0 = c_0 f_c$ in (28) to compare DDM estimation and [10]. However, DDM estimation can handle both *coupled* and *uncoupled* FM signal models because the estimation of the sinusoidal modulation parameters is independent of the polynomial phase parameters.

We note that [10] is based on phase unwrapping, so only phase parameters can be estimated, and shorter signals result in better estimation performance. On the other hand, DDM uses *spectral* estimation, so longer signals yield better performance. The signal length used was $M = 2048$ samples for DDM and $M = 512$ samples for [10]. Additionally, DDM used a 2048-sample *Hann* window spanning the entire signal duration and an FFT with $N = 4096$ samples, whereas the **stage 1** of [10] used a $M = 24$-sample rectangular window and an FFT with $N = 4096$ samples. DDM used $a_0 = 0$ and [10] the corresponding $A = 1$. Note, however, that DDM can estimate the amplitude parameters but [10] cannot. The common parameter values for DDM and [10] used in the MCS presented here are $b_0 = -0.19$ rad, $f_c = 2205$ Hz, $b_2 = 5.03$, $f_0 = 220.50$ Hz, $\phi_0 = 0.72$ rad, and $f_s = 44100$ samples/s. Note that $b_2 > 1$, corresponding to wideband FM.

This section presents the result of 1000 Monte-Carlo simulations (MCS) to compare the accuracy of the proposed estimator against **stage 2** and **stage 3** of the estimator from [10] and the CRLB in noisy conditions. The SNR is defined as $\mathrm{SNR} = {}^{\exp\{2a_0\}}/{\sigma^2}$, where σ^2 is the variance of the additive white Gaussian noise. DDM estimation will be compared to both **stage 2** and **stage 3** from [10]. Fig. 1 shows the minimum squared-error (MSE) of the estimators versus the SNR. The solid line is the *exact* CRLB calculated by inversion of the Fisher information matrix, the dashed line is DDM estimation, the dotted line is **stage 2**, and the dash-dotted line is **stage 3**.

Betser [15] derived the CRLB for the polynomial phase component of the model in (2), whereas the CRLB for the FM sinusoid in (1) can be found in [7, 24]. To avoid numerical problems in the inversion of the Fisher information matrix (FIM) when calculating the CRLB numerically [7], we perform the calculation for $x\left(\frac{n}{M}\right)$ in (28), which corresponds to the following parameter vector $[a_0,\ b_0,\ 2\pi{}^M/{}_{f_s} f_c,\ b_2,\ 2\pi{}^M/{}_{f_s} f_0,\ \phi_0]$. Consequently, we have corrected the CRLB for $\hat{f}_c$ and $\hat{f}_0$ by $({}^{f_s}/{}_{2\pi M})^2$.

5. DISCUSSION

The order of magnitude of the parameters varies from 10^{-1} for ϕ_0 and b_0 up to 10^3 for f_c, so the impact of the MSE of the estimators (and the corresponding CRLB) must be interpreted differently. Note that Figs. (1c) and (1e) show $\hat{f}_c$ and $\hat{f}_0$ in Hz, and that Fig. (1a) only shows DDM because [10] cannot estimate the amplitude.

The bias of an estimator reflects the maximum estimation accuracy that can be achieved with it. Estimation bias typically manifests as the MSE of an estimator no longer following the CRLB, as can be seen in Fig. 1. DDM starts following the CRLB after $\mathrm{SNR} = 0$ dB for almost all FM signal parameters, presenting bias only after $\mathrm{SNR} = 80$ dB for $\hat{f}_0$, $\hat{f}_c$, and $\hat{\phi}_0$. Notably, $\hat{a}_0$, $\hat{b}_0$, and $\hat{b}_2$ do not show estimation bias up to $\mathrm{SNR} = 120$ dB. The estimation of the modulation index b_2 for FM sinusoids is a challenging problem in the literature [7]. **Stage 2** presents bias shortly after $\mathrm{SNR} = 0$ dB, and **stage 3** presents bias consistently *before* DDM.

DDM outperforms **stage 2** above $\mathrm{SNR} = 20$ dB for all parameters due to the bias of **stage 2**. As expected, **stage 3** outperforms DDM estimation for most parameters because **stage 3** uses the estimations from **stage 2** to initialize a nonlinear optimization procedure that achieves quasi-maximum likelihood (QML) performance, which is designed to approximate MLE estimation and approach the CRLB. The implementation of the estimator from [10] used in the MCS shown in Fig. 1 uses the *Nelder-Mead Simplex* (NMS) search algorithm [28].

Table 1: *Comparison of computational complexity of estimators. The table shows the number of arithmetic operations and the estimation time averaged over* 1000 *Monte-Carlo simulations. We are interested in the* relative *estimation time. See text for details.*

Estimator	**Number of Operations**		**Computation Time (s)**
DDM	(FFT) (QR)	$\mathcal{O}(N\log N)$ $\mathcal{O}(K^3)$	7.38×10^{-4}
Stage 2	(FFT) (QR)	$\mathcal{O}(N\log N)$ $\mathcal{O}((2Q+2)^3)$	1.87×10^{-2}
Stage 3	(FFT) (QR) (NMS)	$\mathcal{O}(N\log N)$ $\mathcal{O}((2Q+2)^3)$ $\mathcal{O}(M^2)$	2.29×10^{-2}

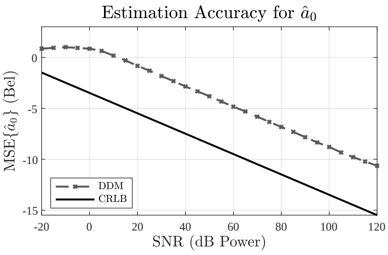

(a) Log amplitude.

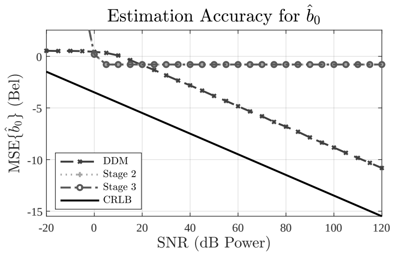

(b) Carrier initial phase.

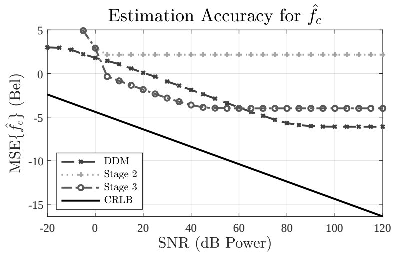

(c) Carrier frequency.

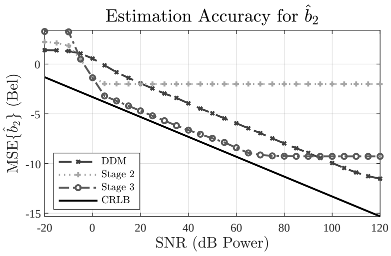

(d) Modulation index.

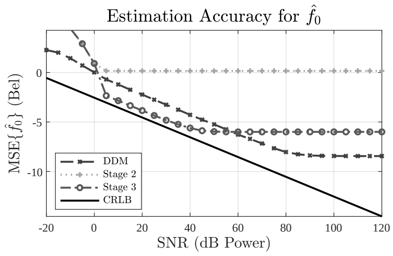

(e) Modulation frequency.

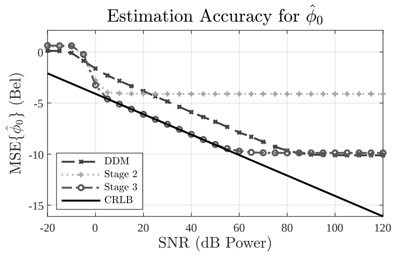

(f) Modulation initial phase.

Figure 1: *Mean-squared error (MSE) of each estimator versus the SNR after* $R = 1000$ *Monte-Carlo simulations. The parameters are* $N = 4096$*, Hann window,* $M = 2048$ *for DDM and* $M = 512$ *for [10],* $a_0 = -0.85$*,* $b_0 = -0.19$ *rad,* $f_c = 2205$ *Hz,* $b_2 = 5.03$*,* $f_0 = 220.50$ *Hz, and* $\phi_0 = 0.72$ *rad, (*$f_s = 44.1\,$*kHz).*

DDM estimation of FM sinusoids is sensitive to the initial estimation of ω_0. Wideband FM signals present spectral peaks at $2\pi f_c + i\,\omega_0$ with high spectral energy according to $J_i\left(b\right)$. Consequently, wideband FM favors estimation of ω_0 using (27) even in noisy conditions, as shown in Fig. (1e), as long as the FM sidebands at integer multiples of ω_0 are above the noise level. Estimation of narrowband FM signals might require exploiting the redundancies in algorithm 1 to overcome the additional challenge of low-energy sideband FM harmonics.

5.1. Computational Complexity

Finally, Table 1 compares the computational complexity of the estimators with regard to both the *number of arithmetic operations* and *computation time* in seconds. The table shows the complexity of individual algorithmic steps, such as the number of operations required to calculate one FFT or one QR decomposition used for the pseudo-inverse. The table also shows an estimation [29] of the complexity of each iteration of the NMS algorithm, which reflects the cost of evaluating the function in eq. (1) and performing least-squares optimization. Thus, in this case, $M = 512$.

DDM estimation described in algorithm 1 uses the FFT with size N and a matrix inversion by QR decomposition. The computational complexity of the QR decomposition algorithm is $\mathcal{O}\left(\chi^3\right)$, where χ is the largest dimension of the rectangular matrix with the coefficients of the system of equations. For **stage 2** and **stage 3**, the model order Q determines χ because there are $2(Q+1)$ parameters to estimate. For DDM, χ is the number of frequency bins used in the estimation, which is the number of bins K around the main lobe of the window in the DFT spectrum. Typically, $K = \lfloor B\, {}^{N}\!/\!{}_{M} \rfloor$, where $\lfloor\cdot\rfloor$ denotes the *floor* operator and B is the width of the main lobe of the window $w\left(t\right)$ in bins when $M = N$ (i.e., no oversampling). For the Hann window used here, $B = 4$ so $K = 8$ when $M = 2048$ and $N = 4096$ used in the simulations. Finally, we note that the window $w\left(t\right)$ chosen also impacts the estimation due to how the main lobe concentrates spectral energy, effectively changing B and *potentially* the estimation performance.

Table 1 also shows the average time in seconds for each estimator. Naturally, time in seconds is highly dependent on the specific machine used for the simulations. However, the **relative** time should be fairly consistent across machines. Therefore, comparing how much longer an estimator takes on average should give an informative illustration of their *relative* performances. Table 1 shows that DDM estimation is faster by two orders of magnitude, taking approximately 4% of the time of **stage 2** and 3% of **stage 3**. Djurović *et al.* [10] state that the most computationally demanding step of their proposed estimator is the FFT, arguing that the other steps can be implemented with less computational complexity. However, **stage 2** comprises several calculations, including multiple QR decompositions, whereas **stage 3** required, on average, more than 60 iterations of NMS with more than 100 function evaluations. This is the tradeoff of estimation accuracy versus computational cost to achieve QML performance.

6. CONCLUSIONS

In this article, we presented an algorithm to estimate all the parameters of frequency-modulated (FM) sinusoids with the distribution derivative method (DDM). The results of Monte-Carlo simulations against additive white Gaussian noise showed that DDM estimation of FM sinusoids has performance comparable to the state of the art. DDM estimation is robust and unbiased for SNR below 80 dB. DDM estimation is relatively simple to implement with the fast Fourier transform (FFT) and its computational complexity is effectively the same. DDM estimation can also estimate the polynomial phase component with arbitrary order.

Future work includes comparing the estimation accuracy and computational complexity of DDM estimation of FM sinusoids with other methods in the literature. We will take advantage of redundancy in the estimation algorithm to improve accuracy and also investigate the impact of the tapering window on estimation performance. DDM estimation can be used to initialize the nonlinear optimization procedure corresponding to **stage 3** in [10]. Additionally, DDM estimation presented here can be easily adapted to other classes of signals, such as sinusoidal [22, 21] or hyperbolic [7] phase. Finally, we will also investigate DDM estimation of the instantaneous amplitude [16] of nonstationary sinusoids.

7. ACKNOWLEDGMENTS

The author would like to thank Julian Neri for the insight about using other sets of linearly independent functions besides polynomials in the signal model of eq. (3) and also for comments on an earlier draft of the manuscript.

8. REFERENCES

[1] John Chowning, "The synthesis of complex audio spectra by means of frequency modulation," *Journal of the Audio Engineering Society*, vol. 21, no. 7, 1973.

[2] Ixone Arroabarren, Miroslav Zivanović, and Alfonso Carlosena, "Analysis and synthesis of vibrato in lyric singers," in *11th European Signal Processing Conference*, 2002, pp. 1–4.

[3] I. Arroabarren, M. Zivanović, J. Bretos, A. Ezcurra, and A. Carlosena, "Measurement of vibrato in lyric singers," *IEEE Trans. Instrumentation and Measurement*, vol. 51, no. 4, pp. 660–665, 2002.

[4] I. Arroabarren, X. Rodet, and A. Carlosena, "On the measurement of the instantaneous frequency and amplitude of partials in vocal vibrato," *IEEE Trans. Audio, Speech, and Language Processing*, vol. 14, no. 4, pp. 1413–1421, 2006.

[5] Jeffrey S. Risberg, "Non-linear estimation of fm synthesis parameters," in *Audio Engineering Society Convention 67*, Oct 1980.

[6] Thomas M. Sullivan, "Estimation of FM synthesis parameters from sampled sounds," M.S. thesis, Massachusetts Institute of Technology, Cambridge, MA, September 1988.

[7] F. Gini and G.B. Giannakis, "Hybrid FM-polynomial phase signal modeling: parameter estimation and Cramer-Rao bounds," *IEEE Trans. Sig. Proc.*, vol. 47, no. 2, pp. 363–377, 1999.

[8] Zhaofa Wang, Yong Wang, and Liang Xu, "Parameter estimation of hybrid linear frequency modulation-sinusoidal frequency modulation signal," *IEEE Signal Processing Letters*, vol. 24, no. 8, pp. 1238–1241, 2017.

[9] Pu Wang, Philip V. Orlik, Kota Sadamoto, Wataru Tsujita, and Yoshitsugu Sawa, "Cramér–Rao bounds for a coupled mixture of polynomial phase and sinusoidal FM signals," *IEEE Sig. Proc. Letters*, vol. 24, no. 6, pp. 746–750, 2017.

[10] Igor Djurović, Pu Wang, Marko Simeunović, and Philip V. Orlik, "Parameter estimation of coupled polynomial phase and sinusoidal FM signals," *Signal Processing*, vol. 149, pp. 1–13, 2018.

[11] Yong Wang and Jian Kang, "Parameter estimation for rigid body after micro-Doppler removal based on L-statistics in the radar analysis," *Journal of Systems Engineering and Electronics*, vol. 26, no. 3, pp. 457–467, 2015.

[12] Rui Zhang, Gang Li, and Yimin Daniel Zhang, "Micro-Doppler interference removal via histogram analysis in time-frequency domain," *IEEE Trans. Aerospace and Electronic Systems*, vol. 52, no. 2, pp. 755–768, 2016.

[13] Li Sun, Qi-Fang He, Ling-Hua Su, and Yong-Zhao Lin, "Precession period estimation using sinusoidal frequency modulated Fourier-Bessel series expansion," in *Progress in Electromagnetics Research Symposium - Fall (PIERS - FALL)*, 2017, pp. 664–670.

[14] Xing Yongchang, Hong Wei, Zhang Heng, Ding Youfeng, Sun Bin, and Hu Wankun, "Parameter estimation of sinusoid frequency modulation signal in heavy-tailed noise," in *2nd Int. Conf. Advances in Computer Technology, Information Science and Communications (CTISC)*, 2020, pp. 46–51.

[15] Michaël Betser, "Sinusoidal polynomial parameter estimation using the distribution derivative," *IEEE Trans. Sig. Proc.*, vol. 57, no. 12, pp. 4633–4645, 2009.

[16] Guotong Zhou, G.B. Giannakis, and A. Swami, "On polynomial phase signals with time-varying amplitudes," *IEEE Trans. Sig. Proc.*, vol. 44, no. 4, pp. 848–861, 1996.

[17] Igor Djurović, Marko Simeunović, and Pu Wang, "Cubic phase function: A simple solution to polynomial phase signal analysis," *Signal Processing*, vol. 135, pp. 48–66, 2017.

[18] Saman S. Abeysekera, "Instantaneous frequency estimation from FM signals and its use in continuous phase modulation receivers," in *7th Int. Conf. Information, Communications and Sig. Proc. (ICICS)*, 2009, pp. 1–5.

[19] Bin Deng, Yu-Liang Qin, Hong-Qiang Wang, Xiang Li, and Lei Nie, "SFM signal detection and parameter estimation based on pulse-repetition-interval transform," in *20th European Sig. Proc. Conf. (EUSIPCO)*, 2012, pp. 1855–1859.

[20] Igor Djurović, Vesna Popović-Bugarin, and Marko Simeunović, "The STFT-based estimator of micro-doppler parameters," *IEEE Transactions on Aerospace and Electronic Systems*, vol. 53, no. 3, 2017.

[21] Guo Bai, Yufan Cheng, Wanbin Tang, Qihang Peng, and Jun Wang, "Estimation of sinusoidal frequency-modulated signal parameters by two branches and two stages," *IEEE Trans. Sig. Proc.*, vol. 68, pp. 4959–4970, 2020.

[22] Xiaodong Jiang, Siliang Wu, Yuan Chen, and Lei Qiu, "Parameter estimation for sinusoidal frequency-modulated signals using phase modulation," *IEEE Sig. Proc. Letters*, vol. 28, pp. 76–80, 2021.

[23] F. Gini and G.B. Giannakis, "Parameter estimation of hybrid hyperbolic FM and polynomial phase signals using the multi-lag high-order ambiguity function," in *31st Asilomar Conf. Sig., Syst. and Computers*, 1997, vol. 1, pp. 250–254.

[24] Pu Wang, Philip V. Orlik, Kota Sadamoto, Wataru Tsujita, and Fulvio Gini, "Parameter estimation of hybrid sinusoidal FM-polynomial phase signal," *IEEE Sig. Proc. Letters*, vol. 24, no. 1, pp. 66–70, 2017.

[25] Jihao Yin, Yun Hua, Wanlin Yang, and Tianqi Chen, "On the use of a linear data model for parameter estimation of sinusoidal FM signals," in *2009 Int. Conf. Communications, Circuits and Systems*, 2009, pp. 387–390.

[26] Laurent Schwartz, *Théorie des Distributions (In French)*, vol. I, Publications de l'Institut de Mathématique de l'Université de Strasbourg, Actualités Scientifiques et Industrielles, no. 9, 1950.

[27] Laurent Schwartz, *Théorie des Distributions (In French)*, vol. II, Publications de l'Institut de Mathématique de l'Université' de Strasbourg, Actualités Scientifiques et Industrielles, no. 10, 1951.

[28] Jeffrey C. Lagarias, James A. Reeds, Margaret H. Wright, and Paul E. Wright, "Convergence properties of the Nelder–Mead simplex method in low dimensions.," *SIAM Journal on Optimization*, vol. 9, no. 1, pp. 112–147, 1998.

[29] Sanja Singer and Saša Singer, "Complexity analysis of Nelder–Mead search iterations," in *Proceedings of the 1st Conference on Applied Mathematics and Computation*, 1999, pp. 185–196.

[30] Dominique Fourer, François Auger, and Geoffroy Peeters, "Local AM/FM parameters estimation: Application to sinusoidal modeling and blind audio source separation," *IEEE Signal Processing Letters*, vol. 25, no. 10, pp. 1600–1604, 2018.

[31] Bo Peng, Xizhang Wei, Bin Deng, Haowen Chen, Zhen Liu, and Xiang Li, "A sinusoidal frequency modulation fourier transform for radar-based vehicle vibration estimation," *IEEE Trans. Instrumentation and Measurement*, vol. 63, no. 9, pp. 2188–2199, 2014.

[32] Pu Wang, Philip V. Orlik, Bingnan Wang, Kota Sadamoto, Wataru Tsujita, and Yoshitsugu Sawa, "Speed estimation for contactless electromagnetic encoders," in *43rd Annual Conference of the IEEE Industrial Electronics Society (IECON)*, 2017, pp. 3340–3344.

[33] Pu Wang, Philip V. Orlik, Kota Sadamoto, Wataru Tsujita, and Fulvio Gini, "Parameter estimation of hybrid sinusoidal FM-polynomial phase signal," *IEEE Signal Processing Letters*, vol. 24, no. 1, pp. 66–70, 2017.

[34] S. Peleg, B. Porat, and B. Friedlander, "The achievable accuracy in estimating the instantaneous phase and frequency of a constant amplitude signal," *IEEE Trans. Sig. Proc.*, vol. 41, no. 6, pp. 2216–2224, 1993.

[35] Pu Wang, Toshiaki Koike-Akino, Milutin Pajovic, Philip V. Orlik, Wataru Tsujita, and Fulvio Gini, "Misspecified CRB on parameter estimation for a coupled mixture of polynomial phase and sinusoidal fm signals," in *IEEE Int. Conf. Acoustics, Speech and Sig. Proc. (ICASSP)*, 2019, pp. 5302–5306.

[36] Stefano Fortunati, Fulvio Gini, and Maria S. Greco, "The constrained misspecified Cramér–Rao bound," *IEEE Sig. Proc. Letters*, vol. 23, no. 5, pp. 718–721, 2016.

[37] Christ D. Richmond and Larry L. Horowitz, "Parameter bounds on estimation accuracy under model misspecification," *IEEE Trans. Sig. Proc.*, vol. 63, no. 9, pp. 2263–2278, 2015.

[38] Robby McKilliam and André Pollok, "On the Cramér–Rao bound for polynomial phase signals," *Signal Processing*, vol. 95, pp. 27–31, 2014.